

Supporting Information

for

Crystal Structures and Solution Properties of Discrete Complexes Composed of Saddle-Distorted Molybdenum(V)-Dodecaphenylporphyrins and Keggin-Type Heteropolyoxometalates Linked by Direct Coordination

Atsutoshi Yokoyama,[†] Takahiko Kojima,^{‡,*} Kei Ohkubo,[†] and Shunichi Fukuzumi^{†,§,*}

Department of Material and Life Science, Division of Advanced Science and Biotechnology, Graduate School of Engineering, Osaka University, Suita, Osaka 565-0871, Department of Chemistry, Graduate School of Pure and Applied Sciences, University of Tsukuba, Tsukuba 305-8571, Japan, and Department of Bioinspired Science, Ewha Womans University, Seoul 120-750, Korea

[†] Osaka University.

[‡] University of Tsukuba.

[§] Ewha Womans University.

* To whom correspondence should be addressed.

E-mail: kojima@chem.tsukuba.ac.jp, fukuzumi@chem.eng.osaka-u.ac.jp

X-ray Crystallography. X-ray crystallography on 1 and 6: All measurements were made on a Rigaku Mercury CCD area detector with graphite monochromated Mo-K α radiation. The data were collected at a temperature of -170 ± 1 (**1**) and -150 ± 1 (**6**) °C to a maximum 2θ value of 55.0° . A total of 1240 oscillation images were collected. A sweep of data was done using ϕ scans from -80.0 to 100.0° in 0.3° step, at $\omega = 0.0^\circ$ and $\chi = 0.0^\circ$. The exposure rate was 33.3 sec/deg. The detector swing angle was 19.80° . A second sweep was performed using ω scans from -20.0 to 28.0° in 0.3° step, at $\chi = 90.0^\circ$ and $\phi = 0.0^\circ$. The exposure rate was 33.3 sec/deg. The detector swing angle was 19.80° . The crystal-to-detector distance was 44.24 mm. Readout was performed in the 0.273 mm pixel mode. All crystallographic data are summarized in Table S1.

X-ray crystallography on 5 and 7: All measurements were made on a Rigaku Mercury CCD area detector with graphite monochromated Mo-K α radiation. The data were collected at a temperature of $-150 \pm 1^\circ\text{C}$ to the maximum 2θ value of 55.0° . A total of 720 oscillation images were collected. A sweep of data was done using ω scans from -70.0 to 110.0° in 0.5° step, at $\chi = 45.0^\circ$ and $\phi = 0.0^\circ$. The exposure rate was 20.0 (**5**) and 48.0 (**7**) sec/deg. The detector swing angle was 20.06° . A second sweep was performed using ω scans from -70.0 to 110.0° in 0.5° step, at $\chi = 45.0^\circ$ and $\phi = 90.0^\circ$. The exposure rate was 20.0 sec/deg. The detector swing angle was 20.06° . The crystal-to-detector distance was 44.54 mm. Readout was performed in the 0.273 mm pixel mode. All crystallographic data are summarized in Table S1.

Structure Refinements. Refinement on F^2 was performed for all reflections. The weighted R factor R_w and goodness of fit S are based on F^2 , and the conventional R factors R on F , with F set to zero for negative F^2 . The threshold expression of $F^2 > 2\sigma(F^2)$ was used only for calculating R factors (gt) etc. and was not relevant to the choice of reflections for refinement. R factors based on F^2 are statistically about twice as large as those based on F , and R factors based on all data are even larger. Since the oxygen and tungsten atoms in the Keggin moieties were disordered in the crystals of **5**, **6** and **7**, each

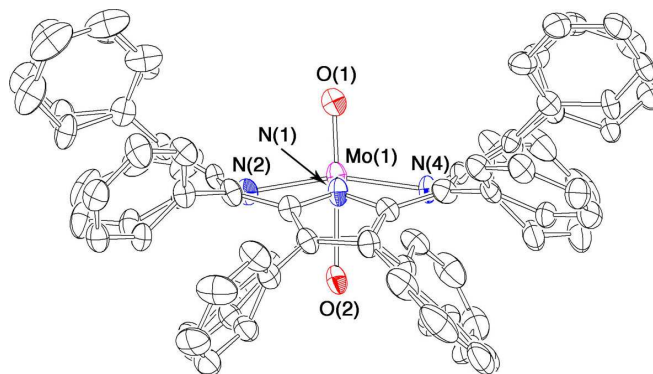
atom was refined isotropically with occupancy of 0.5.

Table S1. Crystallographic Data for **1**, **5**, **6** and **7**.

	1	5	6	7
Formula	C ₉₂ H ₆₂ N ₄ O ₆ Cl	C ₁₈₄ H ₁₂₁ N ₈ O ₄₂ PMo ₂ W ₁₂	C ₁₈₄ H ₁₂₂ N ₈ O ₄₂ SiMo ₂ W ₁₂	C ₁₈₄ H ₁₂₃ N ₈ O ₄₂ BMo ₂ W ₁₂
F. W.	1699.67	5544.95	5543.07	5526.80
crystal system	triclinic	monoclinic	monoclinic	monoclinic
space group	<i>P</i> -1	<i>P</i> 2 ₁ / <i>n</i>	<i>C</i> 2/ <i>m</i>	<i>P</i> 2 ₁ / <i>c</i>
<i>T</i> , K	103	123	123	123
<i>a</i> , Å	15.901(6)	17.607(15)	18.4212(11)	17.750(5)
<i>b</i> , Å	16.509(6)	37.654(10)	37.5328(17)	37.319(9)
<i>c</i> , Å	18.453(7)	18.227(5)	17.8126(11)	18.393(5)
α , deg.	104.143(3)	—	—	—
β , deg.	108.391(3)	118.664(4)	118.897(2)	118.6632(11)
γ , deg.	109.915(3)	—	—	—
<i>V</i> , Å ³	3972(3)	10605(5)	10782(10)	10691(5)
<i>Z</i>	2	2	2	2
No. of reflections	30844	75582	33298	74601
No. of observations	17703	23851	9879	23451
No. of parameters	1019	1099	560	1099
<i>R</i> 1 ^a (<i>I</i> > 2.0σ(<i>I</i>))	0.123	0.135 (0.072°)	0.077	0.158 (0.088°)
<i>wR</i> 2 ^b (all data)	0.338	0.239 (0.143°)	0.165	0.313 (0.236°)
GOF	1.130	1.51 (1.08°)	1.11	1.30 (1.08°)

^a $R1 = \sum |F_o| - |F_c| / \sum |F_o|$.^b $wR2 = [\sum (w(F_o^2 - F_c^2)^2) / \sum w(F_o^2)^2]^{1/2}$.^c Structure refinements using the “Squeeze” method.

(a)



(b)

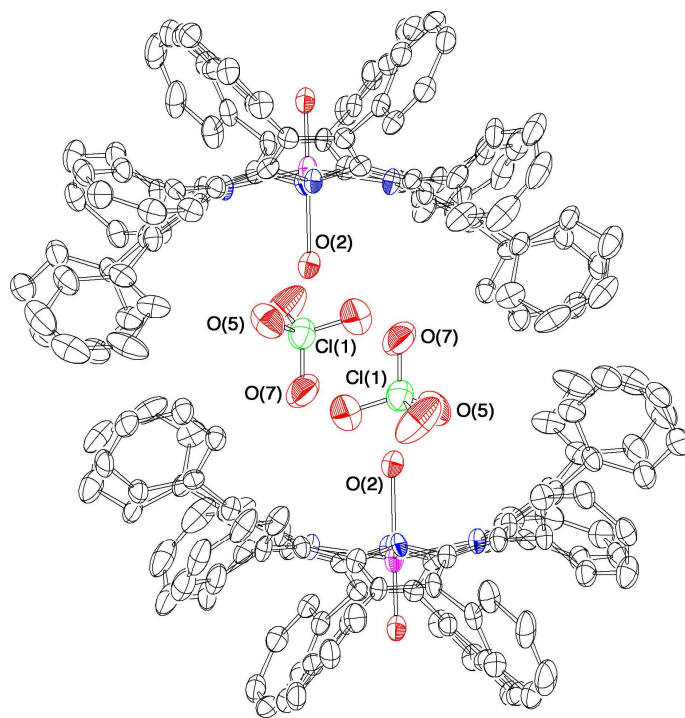
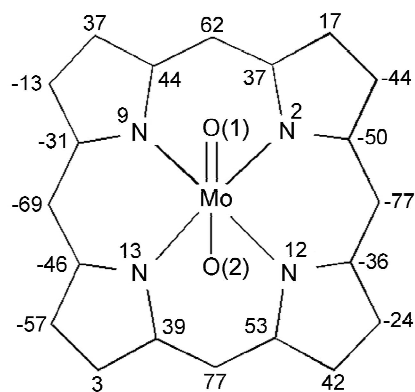
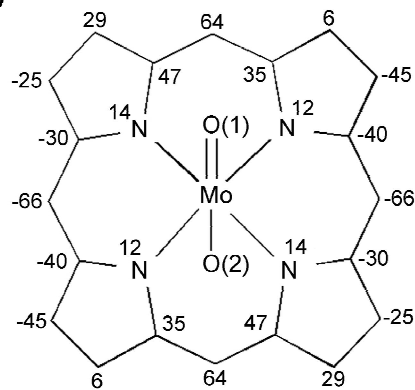


Figure S1. Crystal Structures of $[\text{Mo}(\text{DPP})(\text{O})(\text{H}_2\text{O})]\text{ClO}_4$ (**1**) with 50% probability thermal ellipsoids.

(a)



(b)



(c)

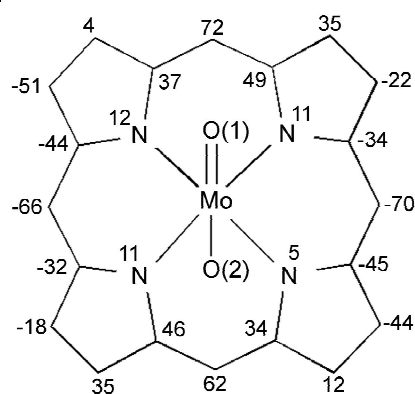


Figure S2. The displacement of each atom from the least-squares mean plane of 24 atoms of the DPP moiety in **5(a)**, **6(b)** and **7(c)** (in units of 0.01 Å).

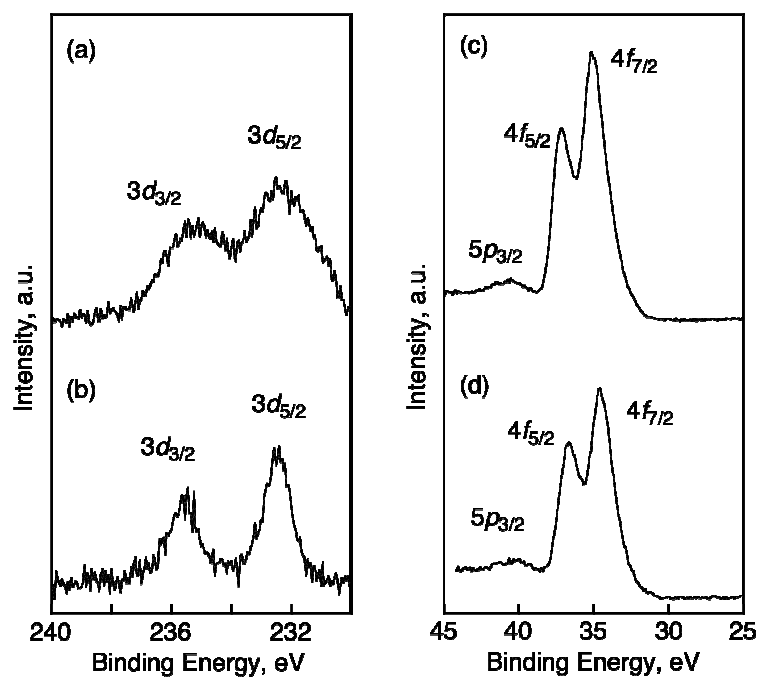


Figure S3. XPS spectra of **1**(a), **3**(c) and **6**(b),(d) in boron nitride pellets. Spectra of (a) and (b) are assigned to Molybdenum atom ($3d_{3/2}$, $3d_{5/2}$). (c) and (d) are assigned to tungsten atom ($5p_{3/2}$, $4f_{5/2}$, $4f_{7/2}$).

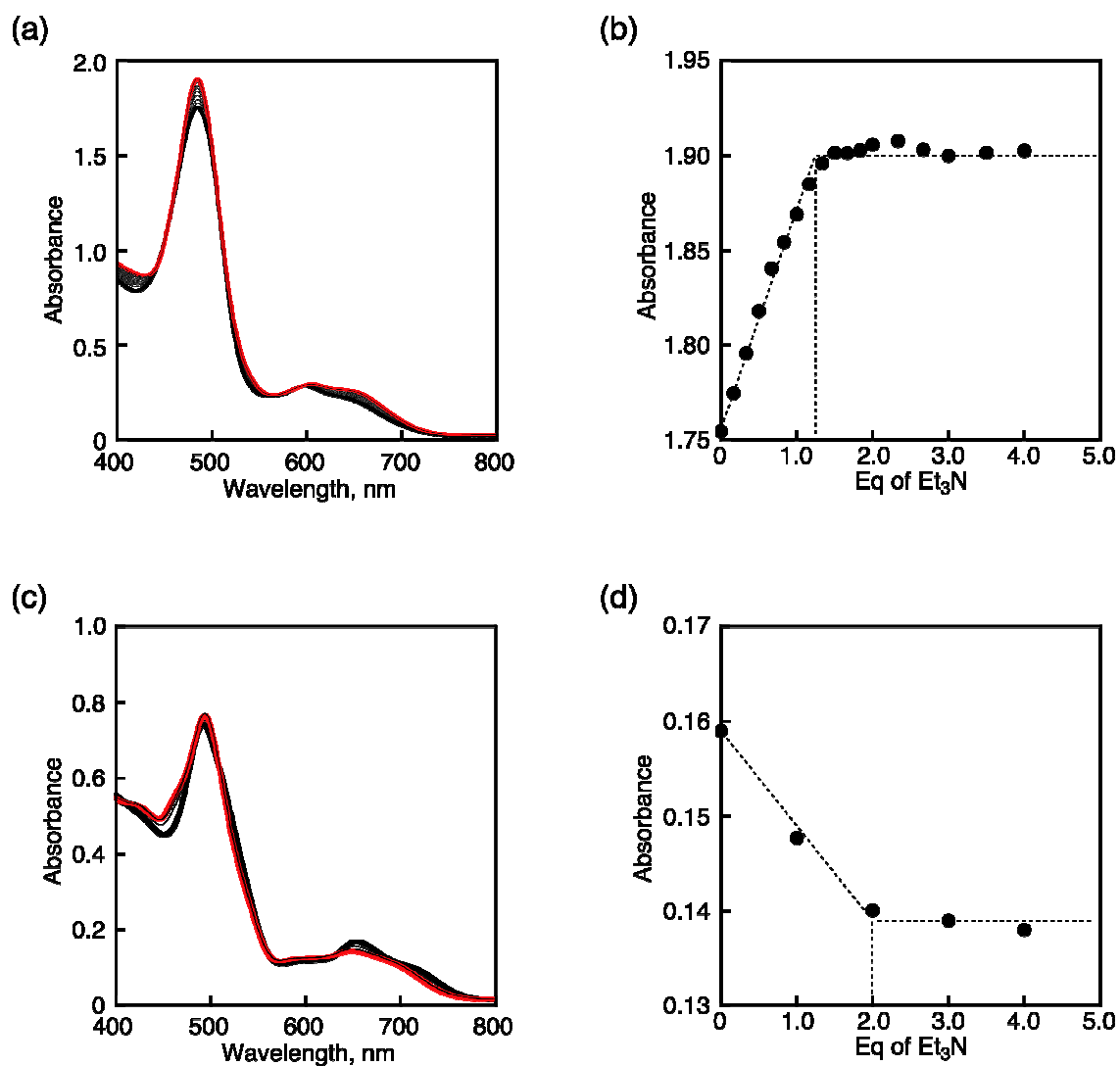


Figure S4. UV-vis spectral changes of (a) **5** (1.0×10^{-5} M) and (c) **6** (1.0×10^{-5} M) upon addition of triethylamine (1 mM). Changes of absorbance at 484.5 nm for **5** (b) and 653 nm for **6** (d) are depicted.

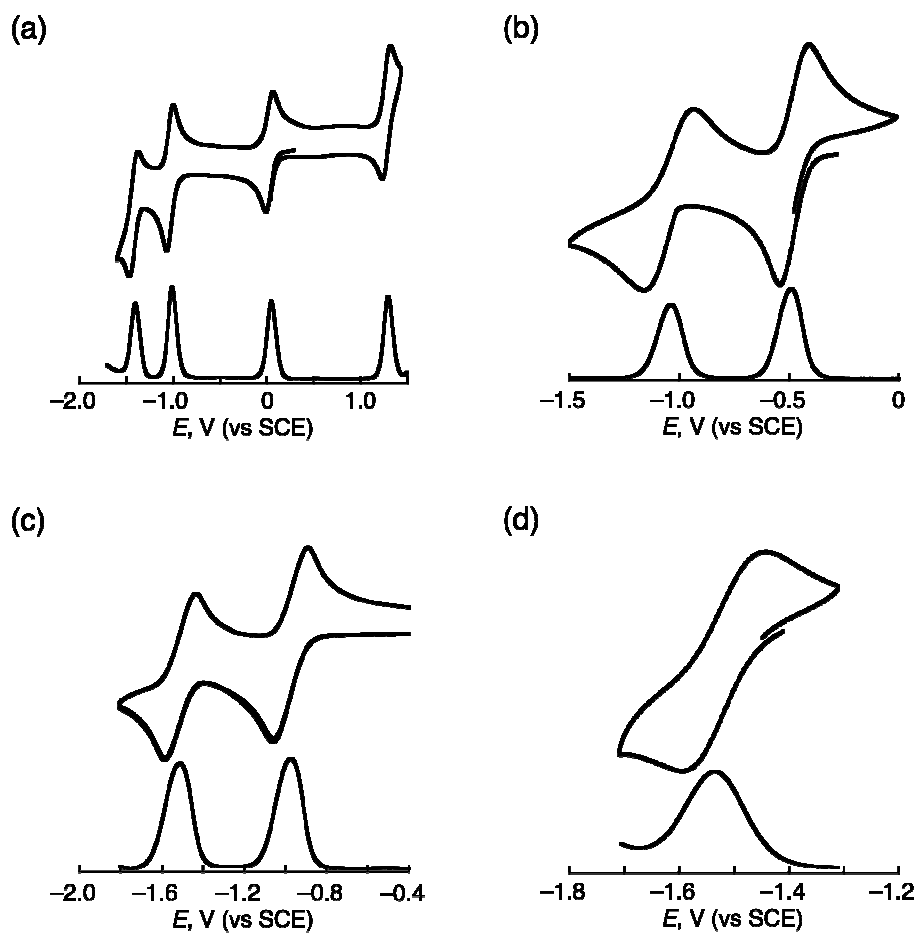


Figure S5. Cyclic voltammograms and differential plus voltammograms for **1**(a), **2**(b), **3**(c), and **4**(d) in PhCN at room temperature under Ar in the presence of 0.1 M TBAPF₆ as an electrolyte.